Talanta 115 (2013) 569–576

Contents lists available at SciVerse ScienceDirect

Talanta

journal homepage: www.elsevier.com/locate/talanta

Fabrication of coated graphite electrode for the selective determination of europium (III) ions

Anjali Upadhyay, Ashok Kumar Singh *, Koteswara Rao Bandi, A.K. Jain

Department of Chemistry, Indian Institute of Technology-Roorkee, Roorkee 247667, India

ARTICLE INFO

Article history:
Received 11 March 2013
Received in revised form
3 June 2013
Accepted 4 June 2013
Available online 19 June 2013

Keywords:
Eu^{3+} selective electrodes
Coated graphite electrode
Ion selective electrode
Potentiometric titration

ABSTRACT

Preliminary complexation study showed that two ligands (ionophores) (2-((2-phenyl-2-(pyridin-2-yl) hydazono)methyl)pyridine) [L_1], (2-((2-phenyl-2-(pyridin-2-yl)hydazono) methyl)phenol) [L_2] can act as europium selective electrode. Europium selective coated graphite electrodes (CGE) were prepared by using ligands [L_1] and [L_2] and their potentiometric characteristics were determined. Membranes having different compositions of poly(vinylchloride) (PVC), the different plasticizers, anionic additives and ionophores were coated onto the graphite surface. The potential response measurements showed that the best performance was exhibited by the proposed CGE. This electrode had the widest working concentration range, Nernstian slope and fast response times of 10 s. The selectivity studies showed that this electrode have higher selectivity towards Eu^{3+} over a large number of cations. Furthermore, the electrode generated constant potentials in the pH range 2.7–9.0. This electrode can be used to quantify europium in soil, binary mixtures and also used as an indicator electrode in the potentiometric titration of Eu^{3+} with EDTA. The proposed electrode was also successfully applied to the determination of fluoride ions in real samples.

1. Introduction

Europium is one of the rare earth elements which is found in minerals xenotime, monazite, and bastnäsite [1]. Europium compounds play an important role in industries because of their special photogenic, magnetic, mechanical and nuclear properties. They are used in production of glass and ceramic, metallurgy, electronics and agriculture and natural sciences. To date more and more europium are getting into the environment as a result of its increasing use in various fields. Continuous exposure to low concentrations of europium together with its toxic effect can cause adverse health effect because of its bioaccumulation along the food chain [2]. Therefore, sensitive, accurate and rapid methods for their separation, purification and determination are of great importance.

A number of instrumental techniques such as adsorption voltammetry [3], multiple square wave voltammetry [4], flow injection chemiluminescence [5], inductively coupled plasma mass spectrometry using flow injection method [6], luminescence spectrometry [7], neutron activation analysis [8], spectrofluorimetric [9], and Second Order Derivative spectrophotometry [10] are available for its estimation. These methods provide accurate determination of europium content but require large infrastructure backup and support of expertise. These requirements make it difficult for such a technique to be used in routine manner for the analysis of a large number of samples. For such a purpose analytical technique which is portable, fast and low cost is the obvious choice. Such requirements are generally met by ion selective electrodes.

These methods are efficient tools for Eu^{3+} detection as they are sensitive and accurate. Unfortunately, their sample pretreatment procedures are time-consuming and require costly and specialized equipment for analysis which may not be available in most laboratories. Ion selective electrodes can analyze large number of samples practically in small time, in the presence of different interferents and can even be adapted to online monitoring. In view of significant advantages of ISE's for analysis, a number of good ISE systems have become commercially available for various chemical species. A number of ISE's for estimation of europium concentration have also been recently reported [11–18]. However they exhibit shortcomings in terms of (i) narrow working concentration range, (ii) non-Nernstian potential response, (iii) narrow pH range and (iv) high response time. These limitations have affected their widespread use in quantification of europium. Thus a more sensitive and selective electrode with good performance parameters for europium quantification is required and needs to be developed. To develop ISE, a selective ionophore is required.

* Corresponding author. Tel.: +91 9412978289.
E-mail addresses: akscyfcy@iitr.ernet.in, akscyfcy@gmail.com (A.K. Singh).

0039-9140/$ - see front matter © 2013 Elsevier B.V. All rights reserved.
http://dx.doi.org/10.1016/j.talanta.2013.06.001

Recently some ligands (ionophores) have been synthesized [19,20] and we have thought it appropriate to notice the possibility of using them as good ionophores for europium (III) ion selective electrodes. In order to understand the affinity of these ligands with different metals, preliminary studies were undertaken. The results showed that these ligands form complexes with a number of metals. Thus preliminary investigations have shown that the ligands form complexes with many metals, but have strong affinity for Eu^{3+} ion. As the ligands show affinity for Eu^{3+} ion, these are likely to act as good ionophores for $Eu^{3+}$and their membrane facilitate the transfer of Eu^{3+} ion as compared to other metal ions. Therefore the two ligands, (2-((2-phenyl-2-(pyridin-2-yl) hydazono)methyl)pyridine) (L_1) and (2-((2-phenyl-2-(pyridin-2-yl) hydazono)methyl)phenol) (L_2) have been chosen as potential ionophores for the preparation of a Eu^{3+} ion selective electrode. Therefore these ionophores were coated on graphite rods and coated graphite electrodes so obtained were studied as Eu(III) selective electrodes. The results presented here show that these electrodes are highly selective for Eu^{3+}.

2. Experimental

2.1. Reagents

Reagent grade sodium tetraphenylborate (NaTPB), potassium tetrakis *p*-(chloro phenyl)borate (KTpClPB), dibutylphthalate (DBP), dioctylphthalate (DOP), acetophenone (AP), 1-chloronapthalene (1-CN), *o*-nitrophenyloctyl ether (*o*-NPOE), tetrahydrofuran (THF) and high molecular weight poly(vinylchloride) were procured from E. Merck (Germany) and used as such. Pyridine-2-aldehyde (Himedia Laboratories Pvt. Ltd., Mumbai, India), salicylaldehyde (SRL, Mumbai, India) were used as obtained. The nitrate and chloride salts of all the cations used were of analytical grade and used without any further purification. The solutions of metal salts were prepared in doubly distilled water and standardized whenever necessary.

2.2. Synthesis of ionophores 2-((2-phenyl-2-(pyridin-2-yl) hydazono)methyl)pyridine (L_1) and 2-((2-phenyl-2-(pyridin-2-yl) hydazono)methylphenol (L_2)

Ionophores L_1 and L_2 were synthesized according to the reported method [19,20]. The structures of ionophores are given in Fig. 1.

2.2.1. Synthesis of 2-((2-phenyl-2-(pyridin-2-yl)hydazono)methyl) pyridine, [L_1]

A solution of 1.445 g (13.50 mmol) of pyridine-2-aldehyde in 5 mL methanol was added to 2.498 g (13.50 mmol) of 2-(1-phenylhydrazinyl)pyridine in 10 mL methanol with continuous stirring. After this reaction mixture was refluxed for 2 h. This reaction mixture was kept at room temperature for overnight. Next day yellow crystals were found at the bottom of the round bottom flask which was filtered and washed with a small amount of methanol and diethyl ether.

Yield: 1.981 g (58.70%). Melting point 145 °C. GC–MS (CH_2Cl_2, m/z): 274 M^+ (5.03%), 196 (100%), 169 (63.31%). IR data (KBr, ν_{max}/cm^{-1}): 1578, $\nu_{C=Nimine}$. UV–visible [CH_2Cl_2, λ_{max}/nm (ε/M^{-1} cm^{-1})]: 240 (8285), 338 (22370). ^{1}H NMR ($CDCl_3$, δ/ppm): 6.71–6.73 (m, 1H), 7.04–7.06 (m, 1H), 7.12–7.15 (m, 2H), 7.12–7.15 (m, 2H), 7.33–7.36 (m, 1H), 7.47–7.48 (*t*, *J*=7.75 Hz, 2H), 7.55–7.64 (m, 3H), 7.96–7.97 (*d*, *J*=8.0 Hz, 1H), 8.05-8.06 (dd, *J*=1.25 Hz, 1H), 8.36-8.37 (m, 1H). ^{13}C NMR ($CDCl_3$, δ/ppm): 157.40, 153.88, 149.19, 147.23, 138.10, 137.21, 136.68, 130.38, 129.42, 128.61, 123.24, 119.26, 116.85, 109.50. Anal. Calcd for $C_{17}H_{14}N_4$: C, 74.43; H, 5.14; N, 20.42, Found: C, 74.38; H, 5.20; N, 20.39.

2.2.2. Synthesis of 2-((2-phenyl-2-(pyridin-2-yl)hydazono) methylphenol, [L_2]

Salicyaldehyde (122.0 mg, 1.00 mmol) and 2-(1-phenylhydrazinyl)pyridine (185.0 mg, 1.00 mmol) were dissolved in 10 mL methanol. The reaction mixture was stirred at room temperature. Within 30 min a white solid began to separate out and stirring was continued for another 2 h. The mixture was stirred for about 2 h, white precipitate was formed. Then it was filtered, washed thoroughly with methanol, diethyl ether and then dried in vacuo. Compound was recrystallized from dichloromethane.

Yield: 145 mg, (50.2%). Melting point, 140–145 °C. IR data (KBr, ν_{max}/cm^{-1}): 3441, ν_{OH}; 1607, $\nu_{C=Nimine}$ and 1297, $\nu_{C\text{-}Ophenol}$. UV–visible [CH_2Cl_2, λ_{max}/nm (ε/$M^{-1}cm^{-1}$)]: 339 (40,163), 310 (27,956), 238 (33,133).1H NMR ($CDCl_3$, δ/ppm): 6.84–6.87 (m, 2 H), 6.96–6.99 (m, 2 H), 7.01–7.03 (*d*, *J*=8.00 Hz, 1H), 7.20–7.24 (td, *J*=6.75 Hz, 2.00 Hz, 1H), 7.29–7.31 (d, *J*=7.50 Hz, 2H), 7.40 (*s*, 1H), 7.52–7.56(*t*, *J*=7.00 Hz, 1H), 7.57–7.61 (td, *J*=6.75 Hz, 2.00 Hz, 1H), 8.27–8.28 (*d*, *J*=5.0 Hz, 1H), 11.73 (*s*, 1H). ^{13}C NMR ($CDCl_3$, δ/ppm): 108.91, 116.69, 116.88, 118.94, 119.26, 129.33, 130.02, 130.15, 130.22, 130.93, 137.69, 137.93, 141.31, 148.43, 156.77, 157.48. Anal. Calcd for $C_{18}H_{15}N_3O$: C, 74.42; H, 5.23; N, 14.52, Found: C, 74.38; H, 5.26; N, 14.45.

2.3. Electrode preparation

Appropriate amounts of membrane components (ionophore, anion additives, PVC and plasticizers) were dissolved in 5 mL of tetrahydrofuran (THF) and the solvent was evaporated to get a concentrated solution. Spectroscopic grade graphite rods (10 mm length and 5 mm diameter) with polished surface were dipped into the solution and withdrawn quickly. The process was repeated several times until a uniform coating formed on the graphite surface. The electrode was allowed to stabilize overnight. Finally the electrode was sealed into a glass tube with epoxy resin. The coating of polymeric membrane electrode on the graphite rod surface was observed by SEM studies (Fig. 2) and it is found that the coating is homogenous throughout the graphite rod.

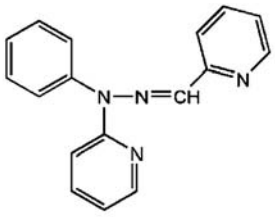

(2-((2-phenyl-2-(pyridin-2-yl)hydazono)methyl)pyridine)
[L_1]

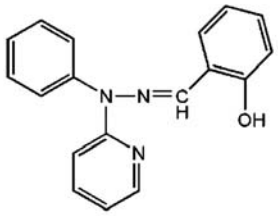

(2-((2-phenyl-2-(pyridin-2-yl)hydazono)methyl)phenol)
[L_2]

Fig. 1. Structure of ionophores (2-((2-phenyl-2-(pyridin-2-yl)hydazono)methyl)pyridine) [L_1], (2-((2-phenyl-2-(pyridin-2-yl)hydazono) methyl)phenol) [L_2].

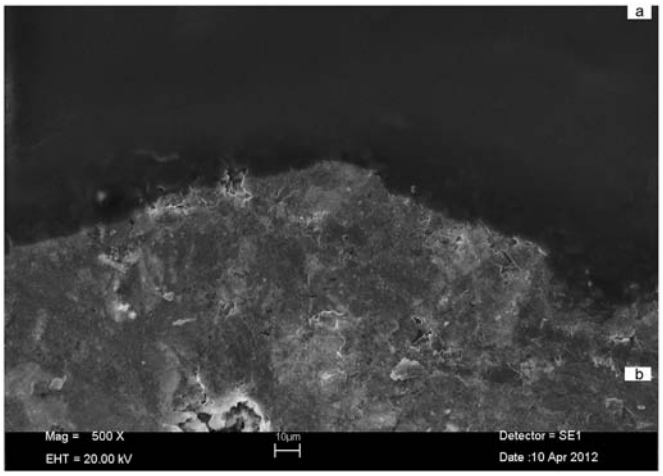

Fig. 2. SEM image of graphite rod (a) with coating and (b) without coating.

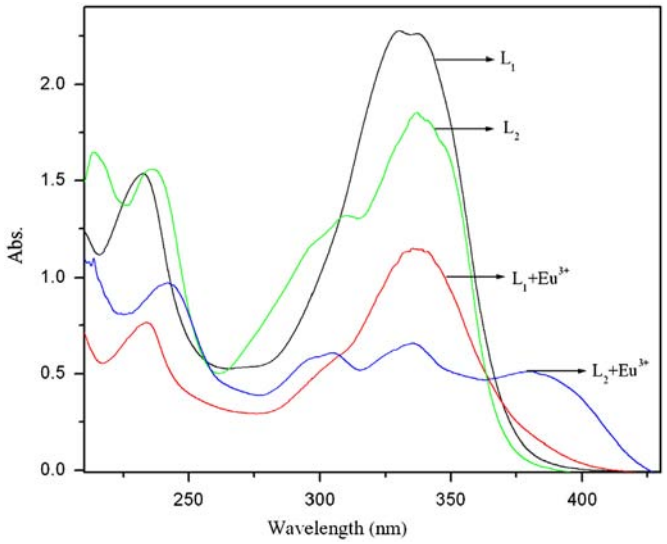

Fig. 3. UV–vis spectral studies of ligands L_1, L_2 (1.0×10^{-4} mol L^{-1}) on the addition of Eu^{3+} ion (1.0×10^{-4} mol L^{-1}).

Such obtained CGE was conditioned in 1.0×10^{-2} M $EuCl_3$ solution for 24 h before potentiometric measurements. The potentials were measured by varying the concentration of $EuCl_3$ solution in the range 1.0×10^{-1} to 1.0×10^{-9} M. Standard $EuCl_3$ solutions were obtained by gradual dilution of 0.1 M $EuCl_3$ solution. The potentials were measured on Century CP 901 digital pH meter at 25 ± 0.1 °C and the following cell was set up.

Coated graphite electrode ‖ test solution ‖ $Hg/HgCl_2$ |KCl (satd.)

Activity coefficients were calculated according to the following Debye–Huckel equation [21]:

$$\log\gamma = -0.511z^2[\mu^{1/2}/(1+1.5\mu^{1/2})-0.2\mu] \quad (1)$$

where μ is the ionic strength and z *is* the valency.

3. Results and discussion

3.1. Complexation study of ionophores L_1 and L_2

In order to confirm the complexation property of the ligands with metals, conductometric studies were also carried out. In this study 20 mL of 1.0×10^{-4} M metal ion solution was titrated with 1.0×10^{-2} M ligand solution and the conductance of the mixture after each addition of ligand, was measured. It is seen that the conductance decreases in the beginning on the addition of the ligand which shows that Eu^{3+} ions are getting complexed with the added ligand. After the completion of complexation reaction, conductance does not change it becomes constant and the break in these plot corresponds to 1:1 (metal to ligand) stoichiometry of the complex. For other metal ions do not show sharp breaks, conductance decreases gradually and does not become constant. Non-constancy in the conductance shows that the formed complexes are weak which then dissociating to produce free metal and ligand. Thus conductometric study also shows that these ionophores have strong affinity for Eu^{3+} and poor for other metals. Thus they can act as good ionophore for Eu^{3+}.

In order to further know the complexation of these ligands for different metals UV–visible study were carried out. For this purpose UV–vis spectra of the metal–ligand mixture were undertaken and spectra for Eu^{3+}–ligand mixture were shown in Fig. 3. UV–vis studies were carried out with 1.0×10^{-4} M of ligand and Eu^{3+} ion solution in methanol. It is seen that the ligands L_1 give three absorption peaks at 209 nm, 232.7 nm, 334.8 nm and ligand L_2 shows four absorption peaks at 213.9, 234.2, 306.3 and 338.1 nm. However on addition of Eu(III) ion solution to the ligands, the peaks shifted due to bathochromic shift and the extra peaks observed only for L_2 at 382.96 nm. This extra peak was due to the MLT (metal to ligand transition) which indicates the formation of metal ligand complex. The observed spectral shifts suggest that the ligand L_2 coordinates more preferentially than L_1 with Eu^{3+} ions. The stoichiometry of the metal complex of ligands (L_1 and L_2) were examined by both Job's method and mole ratio method and the results revealed that stoichiometry of Eu^{3+} ion with ligands (L_1 and L_2) is 1:1.

3.2. Determination of the formation constant

The formation constant of the metal ion–ligand complex is an important parameter for the carrier-based ion-selective electrode, which indicates the practical selectivity of the sensor. The formation constants of the resulting 1:1 metal ion–ligand complex were evaluated by Jobs method, mole-ratio method and also sandwich membrane method. Ligand L_1 is not showing extra peak with metals ions so formation constant for L_1 is not calculated by jobs method and mole ratio method.

3.2.1. Jobs method

Jobs method [22,23] of continuous variation was employed for the determination of formation constant for ligands L_2 with different metal ions. Equimolar solutions (1×10^{-4} M) of ligand L_2 and Eu^{3+} ions were prepared in methanol. Series of solutions of different mole fraction of ligand and metal were prepared and for each solution absorbance was recorded (Fig. 4a). The Jobs plot (absorbance vs. ligand concentration) for L_2 is shown in Fig. 4b at λ_{max}=382.96 nm. and it is observed that maximum absorbance was obtained at mole fraction=0.5 indicating that stoichiometry of europium and L_2 complex is 1:1 and by the Jobs plot the formation constants with different metals were calculated by the following expression:

$$M + L \rightarrow ML \quad (2)$$

$$K_f = \frac{[ML]}{[M][L]} \quad (3)$$

$$K_f = \frac{[A_2/A_1]}{[1-A_2/A_1][C_L - C_M \times A_2/A_1]} \quad (4)$$

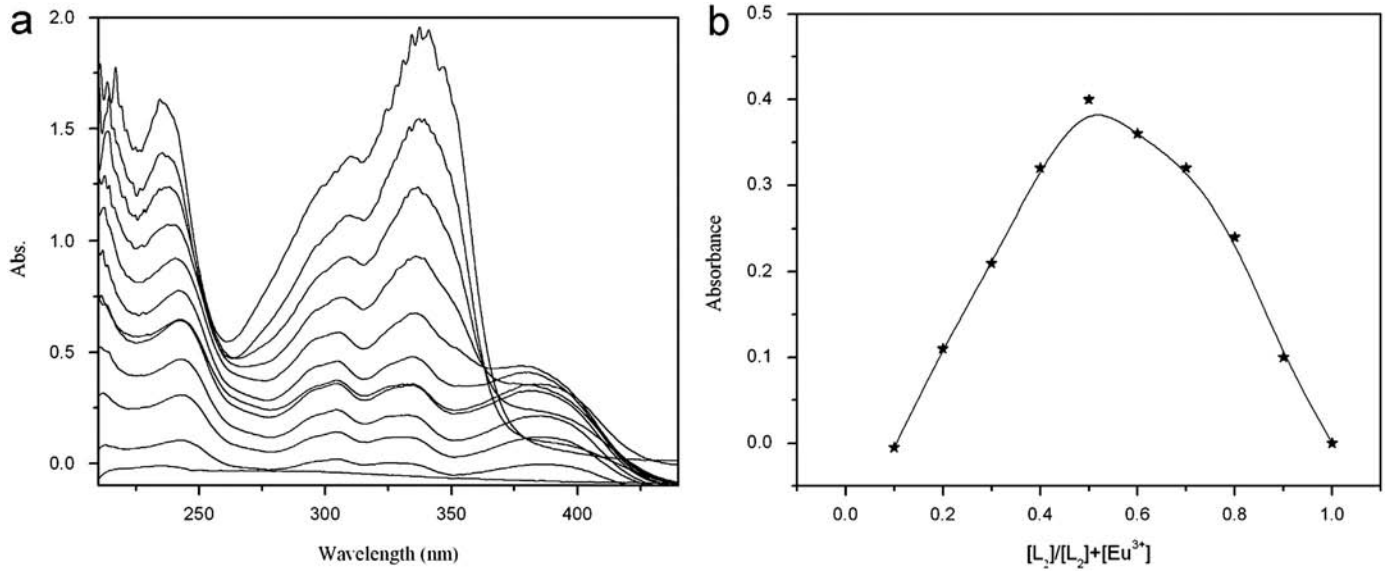

Fig. 4. (a) Variation of UV–vis spectra on addition of series of solutions of different mole fraction of ligand and metal and (b) Job's curve of equimolar concentration (1.0×10^{-4} mol L^{-1}) of ligand L_2 and Eu^{3+}.

where, A_1 is the absorbance at break point, A_2 the actual absorbance, C_M the metal concentration, and C_L the ligand concentration. Formation constant values for L_2 are shown in Table 1.

3.2.2. Molar ratio method

The formation constants were also determined by molar ratio method for L_2 [24]. A series of metal and ligand mixtures with constant ligand concentration and varying metal concentration were prepared and the absorbance of each solution was measured (Fig. 5a) for L_2 of the complexes. The absorbance vs. metal ion concentration plots for Eu^{3+} ion and L_2 is shown in Fig. 5b at λ_{max}=382.96 nm. At higher Eu^{3+} ion concentrations, whole of the ligand has interacted with metal and the europium complex concentration becomes constant resulting in a constant value of absorbance. The break in plot corresponds to stoichiometry of complex. From the break in the plots, the stoichiometry of the complex obtained to be 1:1 and from these molar ratio curves, the formation constants were determined by the following equation:

$$K_f = \frac{C(1-\alpha)}{\alpha C \times (n\alpha C)^n} \quad (5)$$

where C is the total concentration of the complex ion, α is the degree of dissociation and n is the stoichiometry of the complex.

$$\alpha = \frac{(A_2-A_1)}{A_2} \quad (6)$$

where A_2 is the maximum absorbance obtained at intersects of the two lines and A_1 is the absorbance at the stoichiometry ratio of the metal to the reagent in complex. Formation constants for the other metal ions were also determined and tabulated in Table 1.

3.2.3. Sandwich membrane method

The stability constants of the resulting 1:1 metal–ionophore complexes of L_1 and L_2 were also calculated according to sandwich membrane method [25]. The formation constants of various ion–ionophore complexes were evaluated from the following relation:

$$\beta_{IL_n} = \left(L_T - \frac{nR_T}{z_I}\right)^{-n} \exp\left(\frac{E_M z_I F}{RT}\right) \quad (7)$$

where L_T is the total concentration of ionophore in the membrane segment, R_T is the concentration of lipophilic ionic site additives, n is the ion–ionophore complex stoichiometry, E_M is membrane potential, R, T and F are constant having their usual meaning. z_I is the charge on the ion I. The stability constants of different complexes calculated by sandwich membrane method are also given in Table 1.

Table 1
Formation constants of metal complexes with ionophores L_1 and L_2.

Metal ions	Formation constant ($\log \beta_{ILn}$)* ± SD		Formation constant ($\log \beta_{ILn}$)* ± SD	
	Sandwich membrane		Job's method	Mole ratio method
	L_1	L_2	L_2	L_2
Eu^{3+}	**4.45 ± 0.02**	**5.23 ± 0.03**	**5.11 ± 0.02**	**5.46 ± 0.04**
Gd^{3+}	2.95 ± 0.04	3.22 ± 0.03	3.14 ± 0.04	3.17 ± 0.05
Yb^{3+}	2.45 ± 0.03	3.17 ± 0.04	3.03 ± 0.04	3.11 ± 0.03
Co^{2+}	2.57 ± 0.02	2.66 ± 0.03	2.97 ± 0.03	3.01 ± 0.02
Fe^{3+}	2.41 ± 0.02	2.54 ± 0.06	2.84 ± 0.04	2.89 ± 0.03
Cr^{3+}	2.38 ± 0.04	2.44 ± 0.03	2.74 ± 0.03	2.81 ± 0.02
Nd^{3+}	2.22 ± 0.07	2.36 ± 0.02	2.57 ± 0.03	2.62 ± 0.04
Sm^{3+}	2.19 ± 0.04	2.27 ± 0.05	2.34 ± 0.02	2.44 ± 0.03
Tb^{3+}	2.10 ± 0.03	2.19 ± 0.02	2.31 ± 0.03	2.37 ± 0.04
Na^{+}	1.89 ± 0.02	2.09 ± 0.03	2.21 ± 0.02	2.32 ± 0.04
K^{+}	1.78 ± 0.04	1.93 ± 0.03	2.19 ± 0.03	2.11 ± 0.04
La^{3+}	1.65 ± 0.03	1.81 ± 0.04	2.07 ± 0.04	1.92 ± 0.03
Zn^{2+}	1.56 ± 0.04	1.68 ± 0.02	1.82 ± 0.02	1.74 ± 0.03
Er^{3+}	1.43 ± 0.03	1.52 ± 0.04	1.45 ± 0.03	1.34 ± 0.02

The stability constant values obtained from three methods (job's, mole ratio and sandwich membrane method) show that these ligands form most stable complex with Eu^{3+} ion. Whereas the stability constant values for other metal complexes are much smaller, indicating their weak stability. The stability constants value also indicate strongest affinity of ionophores for Eu^{3+} and poor affinity for all other metals listed in Table 1 therefore ionophores are the potential ionophores for pre preparing Eu^{3+} ion selective electrodes.

3.3. Potential response study and optimization of membrane composition

To arrive at optimum composition of the membrane for best performance, first of all potential response having blank membranes with only ionophore L_1 and L_2 was investigated. From the

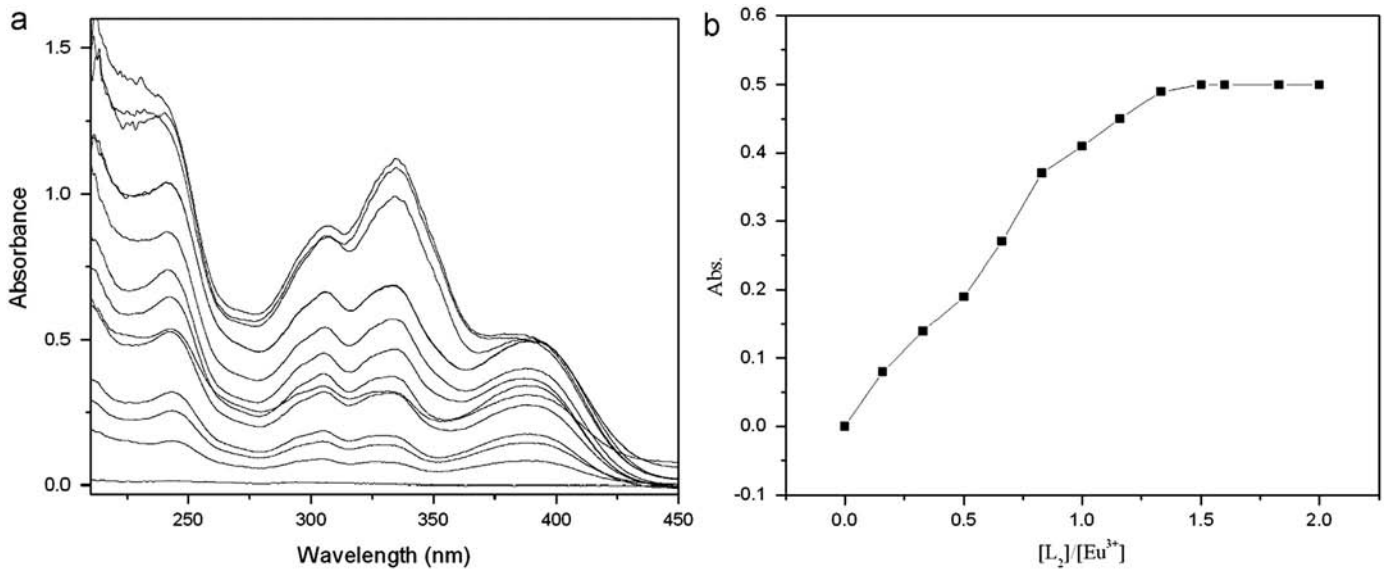

Fig. 5. (a) Variation of UV–vis spectra on addition of series of metal and ligand mixtures with constant ligand concentration and varying metal concentration (b) Molar ratio curve of equimolar concentration (1.0×10^{-4} mol L^{-1}) of ligand L_2 and Eu^{3+}.

potential response plot as a function of log $a_{Eu}{}^{3+}$, membrane performance characteristics were evaluated. It is seen that working concentration range is narrow i.e. 2.5×10^{-4}–1.0×10^{-1} and 3.8×10^{-5}–1.0×10^{-1} mol L^{-1} and slope sub Nernstian as 14.1 ± 0.2 and 15.3 ± 0.3 mV $decade^{-1}$ of activity and high detection limit of 1.8×10^{-5} and 1.3×10^{-5} mol L^{-1} for blank membrane of L_1 and L_2 respectively. These are not good performance characteristics and therefore the performance needs to be improved by changing the composition of the membrane. The membrane composition was changed by the addition of different plasticizers. Sensors having different plasticizers viz. DBP, DOP, AP, 1-CN, *o*-NPOE were prepared and then potential response was investigated. It is seen that performance characteristics of plasticized membrane electrode is better compared to non-plasticized membrane sensors. A perusal of performance characteristics of the plasticized membranes of the two ionophores indicates that the addition of the plasticizers to the membrane widens the working concentration range, increases the slope and lowers the detection limit. The potential response plot confirms that the addition of 1-CN produces best effect as the membrane based on this plasticizer gives the widest working concentration range 1.3×10^{-6}–1.0×10^{-1}, 5.7×10^{-8}–1.0×10^{-1} mol L^{-1}, Nernstian slope 19.8 ± 0.4, 19.5 ± 0.2 mV $decade^{-1}$ of the Eu^{3+} activity and lower detection limit 6.1×10^{-7}, 3.5×10^{-8} mol L^{-1} for sensor of L_1 and L_2 respectively. A comparison of performance characteristics of sensors of L_1 and L_2 shows that the best performance of the sensor is obtained when the relative concentration of NaTPB is lower. Similarly it is seen from that the optimum concentration of the ionophore is 3 and 5 mg for L_1 and L_2 respectively. A comparison of performance of sensors for L_1 and for L_2 shows that better performance of the membrane is achieved with cation excluder NaTPB.

Thus the detailed optimization study of membrane composition revealed that the sensor having compositions L_2:1-CN:NaTPB: PVC as 5:52.5:2.5:40 (w/w; mg), gave the best performance with regard to all performance parameters and therefore this electrode were used for all further studies.

3.4. Dynamic response time behavior of the proposed electrode

It is well known that the dynamic response time of an ion-selective electrode is one of its most important characteristics. To measure the dynamic response time of the electrode the concentration of the test solution was changed in steps from 1.0×10^{-6} M to 1.0×10^{-1} M. The average time required for the electrode to reach a potential response within ± 1.0 mV of the final equilibrium value after successive immersion in a series of Eu^{3+} solution, each increasing in concentration by a factor of 10, was 14 s for CGE–L_1 and 10 s for CGE–L_2. The potentials generated by the electrodes remained stable for about ~5 min after which a slow divergence was recorded.

3.5. Effect of soaking time and lifetime

It is well established that the loss of membrane components due to chemical process at the membrane sample interface is the main cause for the limited lifetime of neutral carrier based ion selective electrodes [26]. To determine the shelf life of the electrodes, their performance was monitored daily over a period of 10 weeks and potential response plots were drawn on daily basis and the performance characteristics measured. No significant change was noticed for 4 weeks for proposed CGE–L_1 and 5 weeks for proposed CGE–L_2. After this period, performance of the electrodes started deteriorating with slope becoming smaller and detection limit higher. However it is important to mention that the electrodes were kept equilibrated with 1.0×10^{-2} mol L^{-1} Eu^{3+} solution when not in use.

3.6. Effect of pH on electrode performance

The pH dependence of proposed CGE–L_1 and proposed CGE–L_2 was examined at 1.0×10^{-3} M concentration of Eu^{3+} ions. The pH of the solution was varied by the small addition of 0.1 M solution of either HCl or NaOH and the potential recorded as a function of pH. The potential remains constant over pH range 3.5–8.5 for proposed CGE–L_1 and 2.7–9.0 for proposed CGE–L_2. Therefore, the same was taken as the working pH range of the electrodes. The significant change in potential response observed at lower pH may be due to the interference of hydrogen ions. On the other hand, the observed potential drift at higher pH values could be due to the hydrolysis of Eu^{3+}.

Table 2
Selectivity coefficients of various interfering ions for Eu^{3+} ion-selective electrodes.

Metal ions	Selectivity coefficient ($K^{Pot}_{A,B}$)	
	CGE–L_2	CGE–L_1
Gd^{3+}	3.09×10^{-4}	1.12×10^{-3}
Yb^{3+}	2.45×10^{-4}	8.12×10^{-4}
Co^{2+}	6.31×10^{-4}	1.69×10^{-3}
Fe^{3+}	1.28×10^{-3}	7.58×10^{-3}
Cr^{3+}	2.75×10^{-3}	8.51×10^{-3}
Nd^{3+}	2.95×10^{-4}	7.58×10^{-3}
Sm^{3+}	5.75×10^{-3}	7.07×10^{-3}
Tb^{3+}	7.58×10^{-4}	2.23×10^{-3}
Na^{+}	1.12×10^{-4}	1.65×10^{-3}
K^{+}	2.08×10^{-4}	5.62×10^{-3}
La^{3+}	1.77×10^{-4}	6.45×10^{-3}
Zn^{2+}	5.42×10^{-4}	1.54×10^{-3}
Er^{3+}	3.25×10^{-3}	4.67×10^{-3}
Cu^{2+}	4.82×10^{-4}	1.44×10^{-3}

Table 3
Potentiometric determination of Eu^{3+} ions from various binary mixtures using proposed CGE–L_2.

Eu^{3+} added (mol L^{-1})	Cation added (mol L^{-1})	Recovery (%)[a]	
		CGE	AAS
5.0×10^{-3}	Gd^{3+}, 5.0×10^{-4}	100.9 ± 0.4	99.2 ± 0.5
5.0×10^{-3}	Nd^{3+}, 5.0×10^{-4}	99.5 ± 0.1	98.9 ± 0.8
5.0×10^{-3}	Yb^{3+}, 5.0×10^{-4}	98.9 ± 0.8	100.1 ± 0.2
5.0×10^{-3}	Tb^{3+}, 5.0×10^{-4}	99.1 ± 0.6	98.3 ± 0.8
5.0×10^{-3}	Sm^{3+}, 5.0×10^{-4}	98.7 ± 0.8	99.4 ± 0.2

[a] Mean value of triplicate measurements.

3.7. Effect of interfering ions on electrode performance

The most important feature of an ISE is its selectivity which is measured in terms of selectivity coefficient. The potentiometric selectivity coefficient values for these electrodes were determined by IUPAC recommended fixed interference method (FIM) [27]. For this purpose, a fixed concentration of interfering ion ($a_B = 1.0 \times 10^{-2}$ mol L^{-1}) was added to the primary Eu^{3+} ion solutions ranging from 1.0×10^{-9} to 1.0×10^{-1} mol L^{-1} and the potentials were measured. The potential values obtained were plotted versus the activity of the Eu^{3+} ion. The linear portions of the potential response curve were extrapolated and the value of $a_{Eu}{}^{3+}$ was obtained from the intersection point. Potentiometric selectivity coefficients were then calculated using the expression:

$$K^{pot}_{Eu^{3+},B} = \frac{\alpha_{Eu^{3+}}}{(\alpha_B)^{z_{Eu^{3+}}/z_B}} \quad (8)$$

The potentiometric selectivity coefficient values given in Table 2 indicate that the electrodes are highly selective to Eu^{3+}. In view of high selectivity towards Eu^{3+}, proposed electrode CGE–L_2 was also used to determine the Eu^{3+} in the various binary mixtures. The binary mixtures were prepared by mixing 5.0×10^{-3} mol L^{-1} solution of Eu^{3+} with 5.0×10^{-4} mol L^{-1} solution of various metal ions such as Gd^{3+}, Nd^{3+}, Yb^{3+}, Tb^{3+} and Sm^{3+}. The recovery of the Eu^{3+} determined from the binary mixture and the values are compared with AAS. The values are tabulated in Table 3, and found that the CGE can be used successfully for the selective determination of Eu^{3+} in various binary mixtures.

Table 4
Response characteristics of Eu^{3+} ion selective CGE–L_1 and CGE–L_2.

Properties	Electrode response	
	CGE–L_1	CGE–L_2
Optimized membrane composition	L_1(3):NaTPB(2):1-CN (53):PVC(44)	L_2(5):NaTPB(2.5):1-CN (52.5):PVC(40)
Soaking time	2 days in 0.01 M $EuCl_3$	2 days in 0.01 M $EuCl_3$
Working concentration range (M)	1.3×10^{-6}–1.0×10^{-1}	5.7×10^{-8}–1.0×10^{-1}
Detection limit (M)	6.1×10^{-7}	3.5×10^{-8}
Slope (mV decade^{-1}of activity)	19.8 ± 0.4	19.5 ± 0.4
Response time (s)	14	10
pH Range	3.5–8.5	2.7–9.0

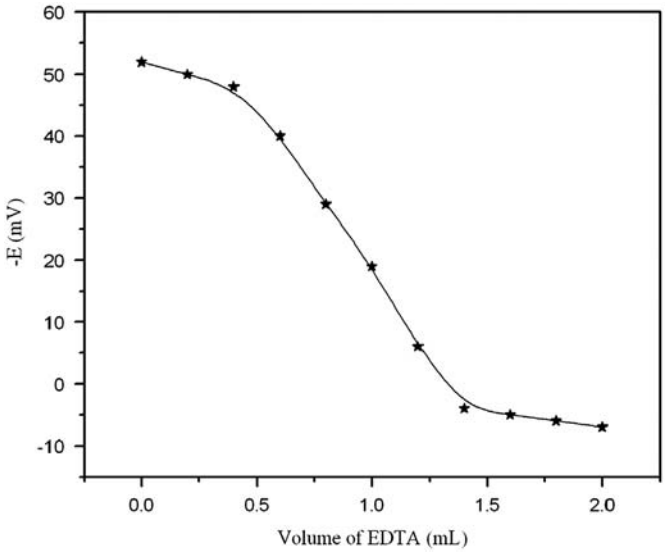

Fig. 6. Potentiometric titration curve of 20 mL of 5.0×10^{-4} M solution of Eu^{3+} ion with 1.0×10^{-2} M EDTA at pH 5.5 CGE–L_2 as indicator electrode.

Table 5
Determination of Eu^{3+} in soil samples by the proposed CGE–L_2.

Samples	CGE[a] (mg Kg^{-1})	AAS[a](mg Kg^{-1})
Soil sample 1 (Haridwar)	1.04 ± 0.03	1.00 ± 0.02
Soil sample 2 (Rishikesh)	1.21 ± 0.04	1.16 ± 0.03

[a] Mean value of triplicate measurements.

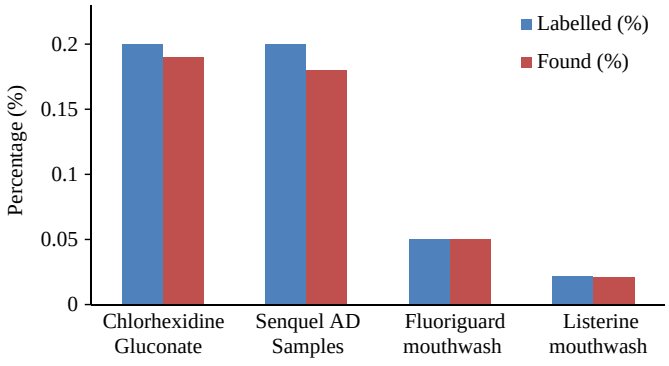

Fig. 7. Determination of fluoride in various samples by the proposed CGE–L_2.

Table 6
Comparison of response characteristics of proposed Eu^{3+} ion selective CGE over with reported electrodes.

Ref. no.	Linear range (M)	Detection limit (M)	Slope (mV decade^{-1} of activity)	pH Range	Response time (s)	Selectivity coefficient ($-\log K^{FIM}_{A,B}$)										
						Gd^{3+}	Yb^{3+}	Co^{2+}	Fe^{3+}	Cr^{3+}	Nd^{3+}	Sm^{3+}	Tb^{3+}	Na^{+}	La^{3+}	K^{+}
[11]	1.0×10^{-5}–1.0×10^{-2}	5.0×10^{-6}	NM	3.0–8.5	5	3.39	3.38	2.95	2.11	2.27	2.18	1.63	2.11	2.27	1.63	1.60
[12]	1.0×10^{-6}–1.0×10^{-2}	6.4×10^{-7}	19.8 ± 0.3	2.4–7.4	<10	3.45	3.49	3.08	2.19	2.27	2.42	2.06	2.14	2.44	2.13	2.11
[13]	1.0×10^{-6}–4.0×10^{-2}	7.2×10^{-7}	19.7 ± 0.5	2.5–9.1	<10	3.18	3.10	3.14	2.31	2.34	–	2.06	2.26	2.37	–	2.24
[14]	4.0×10^{-7}–1.0×10^{-2}	1.5×10^{-7}	18.8 ± 0.2	3.5–8.0	<25	5.13	5.21	–	–	–	4.52	4.55	4.10	4.55	4.18	4.17
[15]	1.0×10^{-6}–1.0×10^{-2}	1.0×10^{-6}	19.7 ± 0.3	3.0–9.5	<6	2.89	2.86	2.97	2.74	2.45	–	2.44	–	3.83	2.62	3.65
[16]	1.0×10^{-6}–1.0×10^{-2}	6.7×10^{-7}	19.5	2.7–8.8	5	3.13	3.06	–	2.65	–	2.25	2.19	3.08	3.45	2.60	2.37
[17]	7.0×10^{-5}–1.0×10^{-1}	5.0×10^{-5}	19.8 ± 0.1	3.0–7.0	<20	–	–	1.53	–	–	–	1.53	1.56	1.58	1.52	1.55
[18]	1.0×10^{-6}–1.0×10^{-2}	4.0×10^{-7}	19.9 ± 0.2	3.5–9.0	10	1.82	3.11	3.29	–	–	–	1.69	2.00	4.79	1.95	4.72
CGE–L_2	5.7×10^{-8}–1.0×10^{-1}	3.5×10^{-8}	19.5 ± 0.2	2.7–9.0	10	3.52	3.61	3.20	2.89	2.56	2.53	2.24	3.12	3.95	2.75	3.68

3.8. Comparison between proposed CGE–L_1 and proposed CGE–L_2

The comparison of performance of two electrodes in Table 4 clearly shows that proposed CGE–L_2 is superior to proposed CGE–L_1 in term of all performance parameters i.e. (i) wide working concentration range (ii) lower detection limit (iii) slope tends more closer to Nernstian value and (iv) wider pH range. Further it is seen from Table 2 that even the selectivity of proposed CGE–L_2 is better than that of proposed CGE–L_1.

4. Analytical applications

4.1. Titration with EDTA

A potentiometric titration of 20 mL of 5.0×10^{-4} M Eu^{3+} ions against 1.0×10^{-2} M EDTA at pH 5.0 was carried out using these electrodes. The titration plots (Fig. 6) is found to be sigmoid shape and the inflexion point of the plot corresponds to 1:1 stoichiometry of Eu–EDTA complex.

4.2. Determination of Eu^{3+} ion in soil

The soil samples (2.0 g) were digested with 10 mL nitric acid. The solution was heated until the evolution of gases stopped. Then a mixture of nitric acid, perchloric acid and conc. hydrofluoric acid (5:3:5) was added followed by controlled heating until evolution of white fumes stopped. After digestion, the residue was removed by filtration and the filtrate was made up to 100 mL. The electrode was used to determine Eu^{3+} in this solution and the results are compiled in Table 5. It is clear from Table 5 that the results obtained by use of electrode are in good agreement with those obtained by AAS.

4.3. Determination of fluoride ion in mouthwash samples

The high selectivity of CGE for Eu^{3+} makes it possible to determine F^- concentration in mouthwash solutions by titrating it with Eu^{3+} solution. A sample of mouthwash solution containing F^- ion was taken and vigorously stirred with water and finally diluted to 100 mL. 25 mL of this solution was titrated with Eu^{3+} solution (1.0×10^{-4} M) at pH 5.5. From the end point of titration plot the concentration of F^- each sample was determined and results are shown in Fig. 7.

5. Comparison with previously reported electrodes

A comparison of the performance characteristics with previously reported electrodes (Table 6) shows that the proposed electrode is superior to the existing electrodes [11–18] in terms of the concentration range, detection limit and selectivity [11–13,15–18]. Therefore, this electrode is an improved addition to the existing set of Europium-selective electrodes. It has been reported that the replacement of inner solution of PME by a solid substance like graphite rod in coated graphite electrode (CGE) inhibits the leakage from internal solution into the test solution and therefore improves the characteristic properties of the electrode along with its selectivity [28]. It was, therefore, decided to prepare a coated graphite electrode for Eu^{3+} ion based on L_2.

6. Conclusions

The studies on a large number of electrodes have shown that of the two ionophores used, the L_2 membranes gave the best performance. The composition of the membrane with the best performance indicators was found to be L_2:1-CN:NaTPB:PVC at a ratio of 5:52.5:2.5:40. This membrane works over a wide working concentration range (5.7×10^{-8} M –0.1 M) in the pH range 2.7–9.0 with a Nernstian slope (19.5 ± 0.2 mV). The response time of the electrode is fast (10 s). With its high sensitivity and selectivity, the electrode could be used for the potentiometric determination of Eu^{3+} in soil and binary mixtures as well as an indicator electrode in the potentiometric titration of Eu^{3+} against EDTA. The proposed electrode was also successfully applied to the determination of fluoride ions in real samples.

Acknowledgment

Ms. Anjali Upadhyay is grateful to Council of Scientific and Industrial Research (CSIR), New Delhi, India for providing financial assistance to undertake this work. I also thank to Dr. Kaushik Gosh for his support in this work.

References

[1] D.R. Lide, CRC Handbook of Chemistry and Physics, 87th ed., CRC Press, Boca Raton, 2006 FL0-8493-0487-3.
[2] P. Liang, B. Hu, Z.C. Jiang, Y.C. Qin, T.Y. Peng, J. Anal. At. Spectrom. 16 (2001) 864–866.
[3] J. Li, S. Liu, X. Mao, P. Gao, Z. Yan J, Electroanal. Chem. 561 (2004) 137–142.
[4] L.M. Moretto, B. Brunetti, J. Chevalet, P. Ugo, Electrochem. Commun. 2 (2000) 175–179.
[5] S. Chen, H. Zhao, X. Wang, X. Li, L. Jin, Anal. Chim. Acta 506 (2004) 25–29.
[6] F. Ardini, F. Soggia, F. Rugi, R. Udisti, M. Grotti, Anal. Chim. Acta 678 (2010) 18–25.
[7] N.M. Sita, T.P. Rao, C.S.P. Iyer, A.D. Damodaran, Talanta 44 (1997) 423–426.
[8] R. Ravisankar, E. Manikandan, M. Dheenathayalu, B. Rao, N.P. Seshadreesan, K. G.M. Nair, Nucl. Instrum. Methods Phys. Res. B 251 (2006) 496–500.
[9] R.D. Bautista, A.I. Jimenez, F. Jimenez, J.J. Arias, Talanta 43 (1996) 421–429.

[10] M. Anbu, T.P. Rao, C.S.P. Iyer, A.D. Damodaran, Chem. Anal. (Warsaw) 41 (1996) 781–785.
[11] M.R. Ganjali, P. Norouzi, A. Daftari, F. Faridbod, M. Salavati-Niasari, Sens. Actuators B 120 (2007) 673–678.
[12] H.A. Zamani, R. Kamjoo, M.M. hosseini, M. Zaferoni, Z. Rafati, M.R. Ganjali, F. Faridbod, S. Meghdadi, Mater. Sci. Eng. C 32 (2012) 447–451.
[13] M.R. Abedi, H.A. Zamani, Eur. J. Chem 8 (2011) S467–S473.
[14] M.R. Ganjali, N. Davarkhah, H. Ganjali, B. Larijani, P. Norouzi, M. Hossieni, Int. J. Electrochem. Sci. 4 (2009) 762–771.
[15] B. Rezaei, A. Hemati, H. Hadadzadeh, IEEE Sens. J. 12 (2012) 914–921.
[16] H.A. Zamani, N. Rohani, M.R. Abedi, S. Meghdadi, J. Chem. Pharm. Res. 3 (2011) 556–560.
[17] M.R. Ganjali, M. Rahimi, B. Maddah, A. Moghimi, S. Borhany, Anal. Sci. 20 (2004) 1427–1431.
[18] P. Norouzi, M. Hosseini, M.R. Ganjali, M. Rezapour, M. Adibi, Int. J. Electrochem. Sci. 6 (2011) 2012–2021.
[19] K. Ghosh, N. Tyagi, P. Kumar, Inorg. Chem. Commun. 13 (2010) 380–383.
[20] K. Ghosh, N. Tyagi, P. Kumar, U.P. Singh, N. Goel, J. Inorg. Biochem. 104 (2010) 9–18.
[21] S. Kamata, A. Bhale, Y. Fukunaga, H. Murata, Anal. Chem. 60 (1988) 2464–2467.
[22] K.R. Bandi, A.K. Singh, Kamaluddin, A.K. Jain, V.K. Gupta, Electroanalysis 23 (2011) 2839–2850.
[23] P. Job, Ann. Chem 9 (1928) 113–203.
[24] K. Geckeler, G. Lange, H. Eberhardt, E. Bayer, Pure Appl. Chem. 52 (1980) 1883–1905.
[25] Y. Mi, E. Bakker, Anal. Chem. 71 (1999) 5279–5287.
[26] U. Oesch, W. Simon, Anal. Chem. 52 (1980) 692–700.
[27] E. Bakker, E. Pretsch, P. Buhlmann, Anal. Chem. 72 (2000) 1127–1133.
[28] J.B. Harrell, A.D. Jones, G.R. Choppin, Anal. Chem. 41 (1969) 1459–1462.